Calculating excess chemical potentials using dynamic simulations in the fourth dimension

Régis Pomès, Elan Eisenmesser, Carol B. Post, and Benoît Roux

Citation: J. Chem. Phys. **111**, 3387 (1999); doi: 10.1063/1.479622
View online: http://dx.doi.org/10.1063/1.479622
View Table of Contents: http://jcp.aip.org/resource/1/JCPSA6/v111/i8
Published by the American Institute of Physics.

Calculating excess chemical potentials using dynamic simulations in the fourth dimension

Régis Pomès[a),b)]
Theoretical Biology and Biophysics Group T-10, Mail Stop K710, Los Alamos National Laboratory, Los Alamos, New Mexico 87545

Elan Eisenmesser and Carol B. Post
Department of Medical Chemistry, Purdue University, West Lafayette, Indiana 47901-1333

Benoît Roux[a),c)]
Départements de Physique et de Chimie, Université de Montréal, C.P. 6128, Succursalle Centre-Ville, Montréal (Québec), Canada H3C 3J7

(Received 22 December 1998; accepted 24 May 1999)

A general method for computing excess chemical potentials is presented. The excess chemical potential of a solute or ligand molecule is estimated from the potential of mean-force (PMF) calculated along a nonphysical fourth spatial dimension, *w*, into which the molecule is gradually inserted or from which it is gradually abstracted. According to this ''4D-PMF'' (four dimensional) scheme, the free energy difference between two limiting states defines the excess chemical potential: At $w=\pm\infty$, the molecule is not interacting with the rest of the system, whereas at $w=0$, it is fully interacting. Use of a fourth dimension avoids the numerical instability in the equations of motion encountered upon growing or shrinking solute atoms in conventional free energy perturbation simulations performed in three dimensions, while benefiting from the efficient sampling of configurational space afforded by PMF calculations. The applicability and usefulness of the method are illustrated with calculations of the hydration free energy of simple Lennard-Jones (LJ) solutes, a water molecule, and camphor, using molecular dynamics simulations and umbrella sampling. Physical insight into the nature of the PMF profiles is gained from a continuum treatment of short- and long-range interactions. The short-range barrier for dissolution of a LJ solute in the added dimension provides an apparent surface tension of the solute. An approximation to the long-range behavior of the PMF profiles is made in terms of a continuum treatment of LJ dispersion and electrostatic interactions. Such an analysis saves the need for configurational sampling in the long-range limit of the fourth dimension. The 4D-PMF method of calculating excess chemical potentials should be useful for neutral solute and ligand molecules with a wide range of sizes, shapes, and polarities. [S0021-9606(99)51231-2]

INTRODUCTION

Free energy calculations based on computer simulations constitute a powerful tool to compute the excess chemical potential of small molecules in dense fluids[1] and the binding affinities of molecular ligands to biomolecules.[2,3] In such approaches, the relative free energy of two states of the system is obtained by calculating the reversible thermodynamic work from one state to the other. More specifically, the Hamiltonian of the system is written as $H(\lambda)=(1-\lambda)H_0+\lambda H_1$, where H_0 and H_1 are the Hamiltonians for the initial and final thermodynamic states, respectively, and λ is a coupling parameter which yields H_0 at $\lambda=0$ and H_1 at $\lambda=1$. To calculate the excess chemical potential of a molecule, H_1 and H_0 may correspond to states where the molecule is, respectively, coupled and uncoupled to the rest of the system. The Hamiltonian may then be rewritten as $H(\lambda)=H_0+\lambda V_{vu}$, where V_{vu} is the potential energy for solvent–solute interactions. Sampling of the configurational space for discrete values of λ ranging from zero to one (or one to zero) amounts to gradually inserting (or removing) the molecule from the system while maintaining thermodynamic equilibrium. By integrating the expectation value of the derivative of $H(\lambda)$ with respect to λ (so-called ''thermodynamic integration''), or by computing the expectation value of $\exp(-\lambda V_{vu})$ (''thermodynamic perturbation''), one can compute the work required for the insertion into (or abstraction from) the system of interest.

Linear scaling of V_{vu}, however, is fraught with a long-recognized statistical problem associated with the repulsive part of the Lennard-Jones (LJ) potential, namely, the numerical instability resulting from the singularity due to the presence of an infinitely small and infinitely repulsive body in a dense medium at small values of λ.[4] Therefore, alternative coupling schemes are required. Scaling by exponential powers of the coupling parameter, λ^n (where $n>1$), improves the statistical accuracy of the calculation by increasing the

a)Authors to whom correspondence should be addressed.
b)Telephone: +1 505 665 9930; Fax: +1 505 665 3493; Electronic mail: regis@lanl.gov
c)Telephone: +1 514 343 7105; Fax: +1 514 343 7586; Electronic mail: rouxb@plgcn.umontreal.ca

relative amount of configurational sampling at small values of the coupling parameter λ, but it does not remove the instability problem.[5] Effective ways to bypass the problem were reported by Zacharias *et al.*[6] and by Beutler *et al.*[5] The first method consists of combining linear scaling of the LJ energy term with the translation of the effective distances separating the solute from the solvent atoms. In this so-called ''separation-shifted potential scaling'' (SSPS) approach, the LJ potential-energy function for solvent–solute interactions

$$V(r)=4\epsilon\left[\left(\frac{\sigma}{r}\right)^{12}-\left(\frac{\sigma}{r}\right)^{6}\right], \tag{1}$$

where ϵ and σ are the LJ parameters, is replaced by

$$V(r,\lambda)=4\epsilon\left\{\left[\frac{\sigma^2}{r^2+\delta(1-\lambda)}\right]^6-\left[\frac{\sigma^2}{r^2+\delta(1-\lambda)}\right]^3\right\}, \tag{2}$$

where $\delta(1-\lambda)$ is a parametric function varying from 0 for a fully interacting solute (at $\lambda=1$), to a nonzero finite value δ in the decoupling limit ($\lambda=0$).[6] The second method[5] is similar: In that approach, scaling is achieved with a power of λ, and (σ/r) is replaced by $[f(\lambda)+(r/\sigma)^s]^{-1/s}$, where $f(\lambda)$ is a quadratic function of the coupling parameter λ, and s is an integer greater than 1. The advantage of such procedures is to replace the infinitively repulsive ''hard core'' of the LJ potential by a finite potential energy barrier, or ''soft core,'' whose magnitude smoothly decreases to zero in the limit of complete decoupling. These approaches have been applied to calculations of the hydration free energy of neon and ethanol,[6] to an atomic fluid,[7] and to the calculation of the binding free energy of camphor in cytochrome P450.[8]

Furthermore, two methods for improving the efficiency of the coupling parameter approach in free energy calculations were proposed recently. The first one consists in adding an unphysical fourth dimension to the conformational space of the system. The technique was first proposed for efficient conformational sampling of proteins[9] and extended to free energy calculations with the application to an atomic liquid.[7] This approach effectively modifies the potential-energy surface of the system and in particular, circumvents large energy barriers separating thermodynamic states, thereby improving the efficiency of free energy calculations.

Concurrently, the ''λ-dynamics'' free energy simulation technique introduced by Kong and Brooks[10] treats the coupling parameter λ as another degree of freedom of the system rather than as a preset parameter. The advantage of the λ-dynamics technique is that free energy changes can be obtained from potential of mean-force (PMF) calculations in which the dynamics of the system is governed by an extended free energy surface and biasing potentials can be used to overcome free energy barriers. Recently the usefulness of the method was demonstrated for competitive ligand binding.[11,12]

The general method that we propose combines key aspects of each of the three approaches reviewed above for the calculation of excess chemical potentials. First, we note that the shifting of the effective interatomic separation in the LJ potential interactions of the molecule of interest with the rest of the system, Eq. (2), is formally analogous to, and suggests, introducing an extra spatial dimension to the configurational space available to the molecule. Thus, this shifting parameter can be replaced by the extension of the molecule into an unphysical ''fourth dimension,'' in the spirit of Beutler and van Gunsteren's work.[7] By keeping the rest of the system confined to the physical three-dimensional space and allowing the molecule of interest to evolve in the four-dimensional space, one can compute the chemical potential as the PMF or work for moving the molecule along the fourth dimension into which the molecule is gradually inserted, or from which it is gradually abstracted. In this 4D-PMF scheme, the coupling of the molecule of interest to the solvent is treated dynamically, similar to the λ-dynamics approach.[10]

In the following sections, the theoretical foundations of the 4D-PMF method are outlined, and its implementation in molecular-dynamics simulations is summarized. Applications to calculations of the hydration free energy of simple LJ spheres, of water, and of camphor are presented to illustrate the tractability of the method. The PMF profiles are analyzed in terms of surface area laws and solvent-continuum approximations. The applicability and reliability of the method are discussed. Finally, further applications of the method are suggested.

THEORY

A single molecular solute immersed in a bulk solvent is considered. While the solvent atoms evolve in the physical three-dimensional space, the Hamiltonian of the system is extended such that the solute atoms evolve along an unphysical fourth dimension w_u, in addition to the three physical dimensions. We write the total Hamiltonian of the extended system as

$$H=T_v+T_u+V_{vv}+V_{uu}+V_{vu}, \tag{3}$$

where T_v and T_u are the kinetic energy of the solvent and solute atoms, respectively, and V_{vv},V_{uu},V_{uv} are the solvent–solvent, solute–solute, and solvent–solute potential energy. Note that in applications to biomolecular studies, the ''solvent'' degrees of freedom could include those of a protein receptor or binding site. The coordinates of the solvent atoms are $\mathbf{r}_v^{(1)},\mathbf{r}_v^{(2)},\ldots$, where each vector $\mathbf{r}_v^{(i)}\equiv(x_v^{(i)},y_v^{(i)},z_v^{(i)})$ represents the three Cartesian degrees of freedom of solvent atom i. The four cartesian degrees of freedom of atom i of the solute are represented by the vector $\mathbf{r}_u^{(i)}\equiv(x_u^{(i)},y_u^{(i)},z_u^{(i)},w_u)$. For the sake of simplicity, we shall write $\{\mathbf{r}_v\}$ and $\{\mathbf{r}_u\}$ to represent all the solvent and solute coordinates, respectively. The kinetic energy of the solute is

$$T_u=\sum_i\frac{1}{2m_u^{(i)}}((p_{ux}^{(i)})^2+(p_{uy}^{(i)})^2+(p_{uz}^{(i)})^2)+\frac{1}{2M_u}p_{uw}^2, \tag{4}$$

where $M_u=\Sigma_i m_u^{(i)}$ is the total mass of the solute. Since each atom of the solvent interacts with the solute atoms through a superposition of pairwise radially symmetric LJ and coulombic energy functions, the potential-energy V_{vu} is easily extended to account for motion in the fourth dimension by writing any solvent–solute interatomic distance as $\sqrt{(x_v^{(i)}-x_u^{(j)})^2+(y_v^{(i)}-y_u^{(j)})^2+(z_v^{(i)}-z_u^{(j)})^2+w_u^2}$. Following

this prescription, we note that V_{vu} goes to zero when $w \to \infty$, and that it is equal to the normal physical solvent–solute interaction when $w=0$. Thus these two states correspond, respectively, to noninteracting solvent and solute, and to a fully interacting, physical three-dimensional system where the solute is completely immersed in the solvent.

The partition function of the extended system comprises a complete integration over the coordinates and momenta of the solvent atoms evolving in the physical three-dimensional space, as well as those of the solute, which is evolving in four dimensions. The equilibrium probability distribution of the solute along the fourth dimension, $\langle \rho(w) \rangle$, is given by

$$\frac{\langle \rho(w) \rangle}{\langle \rho(w_0) \rangle} = \frac{\int d\{\mathbf{r}_v\} d\{\mathbf{r}_u\} \delta(w_u - w) e^{-\beta(V_v + V_{vu})}}{\int d\{\mathbf{r}_v\} d\{\mathbf{r}_u\} \delta(w_u - w_0) e^{-\beta(V_v + V_{vu})}}, \tag{5}$$

where w_0 is an arbitrary reference point and $\beta^{-1} = k_B T$ is the thermal energy at temperature T (note that all integrals over the cartesian momenta of the solute and solvent cancel out from such configurational averages, including that of the fourth dimension p_{uw}). According to the reversible work theorem

$$W(w) - W(w_0) = -k_B T \ln\left[\frac{\langle \rho(w) \rangle}{\langle \rho(w_0) \rangle}\right], \tag{6}$$

where $W(w)$ is the PMF along the coordinate w,

$$\frac{dW(w)}{dw} = \left\langle \left(\frac{\partial V_{vu}}{\partial w_u} \right) \right\rangle_{(w_u = w)}. \tag{7}$$

Integrating from ∞ to 0 yields the excess chemical potential of the solute, $\Delta\mu_{ex}$,

$$\Delta\mu_{ex} = \int_{\infty}^{0} dw \left\langle \left(\frac{\partial V_{vu}}{\partial w_u} \right) \right\rangle_{(w_u = w)} = W(0) - W(\infty). \tag{8}$$

In practice, $W(\infty)$ will be approximated from sufficiently large values of w, for which the interaction energy of the solute with the rest of the system becomes negligible. In the Appendices, we shall show how, in homogeneous systems, the large-w tail of the PMF can be obtained analytically from a continuum approximation and how the short-range PMF of LJ particles relates to the solvent-exposed area.

In conclusion, by sampling the four-dimensional space, one can follow a reversible pathway for the abstraction of the solute from the solvent—or inversely, its incorporation into the solvent. Such a process amounts to calculating the PMF of the solute in the fourth dimension, between $w=0$ and $w=\infty$. In this 4D-PMF approach, the traditional thermodynamic coupling parameter λ used in free energy perturbation is replaced by allowing dynamical motions along a single, nonphysical degree of freedom w accessible to the solute only and perpendicular to the other cartesian degrees of freedom defining the physical three dimensions of the system.

APPLICATIONS

The PMF for abstraction of LJ particles and of water from bulk water into the fourth dimension, as well as that for insertion of a larger polyatomic solute, camphor, were calculated using Langevin molecular-dynamics simulations with umbrella sampling. The CHARMM program[13] was modified to include the following options. The molecular system was separated in two groups: The solvent, which is evolving in the physical three-dimensional (3D) space, and the solute, which can evolve in four dimensions. The potential energy for the nonbonded interactions of the solute with the solvent was calculated in four dimensions, as indicated in the previous section. The velocity, acceleration, and force vectors of the solute atoms were augmented to include a four-dimensional component. The trajectories were generated by Langevin dynamics at 300 K. In the case of polyatomic solutes, a holonomic constraint was used to impose a single value of w for each atom of the solute at a given time. In the integration of the equations of motion, the acceleration of each solute atom i in the fourth dimension, $m_i^{-1}(-\partial V_{vu}/\partial w^{(i)})$, was replaced by the sum of the forces acting on all the atoms in the fourth dimension, $\Sigma_j(-\partial V_{vu}/\partial w^{(j)})$ divided by the total mass of the solute, $M_u = \Sigma_j m_j$. This procedure ensured energy conservation.

The first system studied consisted of a spherical droplet of 151 water molecules with an argon atom in its center. The TIP3P water potential-energy parameters[14] were used, while the potential-energy interaction of Ar with water was modeled with a LJ potential ($\epsilon = 0.190\,226$ kcal/mol, $\sigma = 3.280\,29$ Å) derived from Berthelot mixing rules[13] from TIP3P[14] and Ar[15] LJ parameters. The spherical solvent boundary potential (SSBP) was imposed to mimic the influence of bulk solvent.[16] A quadratic restraining potential $V(r_u) = \frac{1}{2}k(x_u^2 + y_u^2 + z_u^2)$ (with $k = 10$ kcal/mol/Å^2) was applied to the center-of-mass of the solute to keep it near the center of the hydration droplet in the physical three dimensions. After equilibration in 3D, a series of 21 calculations (windows) was performed. In each window, the solute was subjected to a harmonic (''umbrella'') potential $U_i(w) = \frac{1}{2}k_i(w - w_i)^2$ acting in the fourth dimension alone, where k_i is a force constant and w_i is the reference value of w for window i. The force constant of this biasing potential was $k_i = 5.0$ kcal/mol/Å^2. The reference value varied from $w_i = 0.0$ to 10.0 Å in increments of 0.5 Å. The time step for integration of the equations of motion was 2 fs. In a first series of simulations, the different windows were equilibrated for 5 ps and run for a further 20 ps. In that initial series of simulations, the last configuration of the previous window was used as the starting configuration for the next window. Each window was then extended by a further 80 ps, for a total of 100 ps of production per window (grand total of 2.1 ns), from which the 4D (fourth-dimensional) value of Ar, w_{Ar}, was recorded at every time step. The resulting probability distribution of Ar in the fourth dimension was then computed and debiased using the weighted histogram analysis method (WHAM).[17,18] This yielded the PMF for the abstraction of Ar from water. The same procedure was used with a larger LJ sphere ($\epsilon = 0.190\,226$ kcal/mol; $\sigma = 4.613\,25$ Å).

To calculate the PMF for abstraction of a solute water molecule, the same methodology was used with a droplet of 151 TIP3P water molecules as a starting point. The simulation consisted of 22 umbrella runs, with reference w_i varying in increments of 0.5 Å from -0.5 to 10 Å with a force constant of 5 kcal/mol/Å^2.

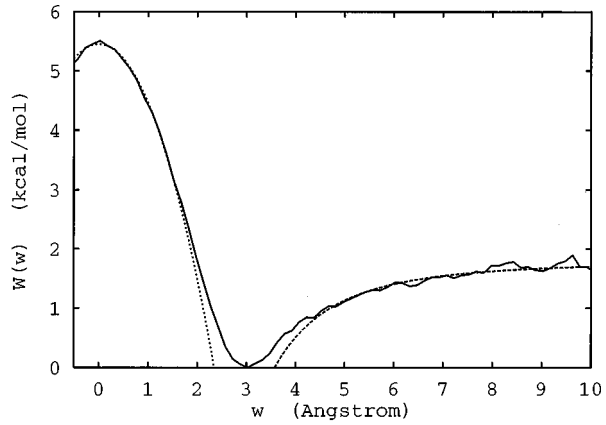

FIG. 1. (——) PMF calculated for the abstraction of Ar from water along the fourth dimension w ($\epsilon=0.190\,226$ kcal/mol, $\sigma=3.2809$ Å). The solute is fully interacting at $w=0$ and completely decoupled in the limit $w=\pm\infty$. (----) short-range fit $f_{\mathrm{SR}}=-0.99w^2+5.45$; (– – –) long-range fit $f_{\mathrm{LR}}=-81.4w^{-3}+1.78$.

Finally, the PMF for insertion of a camphor molecule into the water droplet was calculated from 22 windows with $k_i=5.0$ kcal/mol/Å^2, and successive reference values spaced by 0.5 Å between $w_i=8.0$ and 2.5 Å, and spaced by 0.25 Å between 2.5 and 0.0 Å. The smaller spacing between successive windows at small values of w was designed to increase statistical sampling in the steep region of the PMF corresponding to insertion of the repulsive cores of the camphor atoms. Equilibration of each window consisted in sequential runs of 10 ps. The production or data-collection part of the calculation consisted in simulations of 40 ps performed concurrently on four R-10 000 SGI processors. The total simulation time of 1.1 ns took a total of ~40 h of CPU. The equilibrium geometry and internal-energy parameters of camphor were as listed by Helms and Wade.[19] The LJ parameters were taken from the CHARMM force field, version 22,[20] by assigning the atom types C and O to the keto atoms, and the types CT, CT1, CT2, and CT3 to the remaining C atoms bearing respectively 0, 1, 2, and 3 H atoms. The partial charges of the keto group were $0.38e$ and $-0.38e$ for C and O, respectively;[19] the partial charges of all H atoms were $0.09e$, and those of each of the nonketo C atoms were given by $-n\times0.09e$, where n is the number of coordinating H atoms.

RESULTS AND ANALYSIS

Simple Lennard-Jones solutes

The PMF for abstraction of Ar from bulk water into the fourth dimension w is plotted in Fig. 1. This profile has three distinct regions. In the short range ($w<2$ Å), the PMF assumes the shape of a quadratic barrier centered at the origin. The barrier arises because at small values of w the PMF is dominated by strongly repulsive forces (the LJ core) which tend to expel the solute into the fourth dimension. This short-range (SR) part of the PMF profile can be fit well by a harmonic function $f_{\mathrm{SR}}(w)=5.45-0.99w^2$ kcal/mol (see Fig. 1). In Appendix A, it is seen that this quadratic dependence can be interpreted in terms of a phenomenological solvent-exposed area law by considering the w-dependence of the three-dimensional distance of closest approach between solute and water atoms. From Eq. (A5), the above fit corresponds to an apparent surface tension $\gamma=0.99/(4\pi)=0.0788$ kcal/mol/Å$^2=54.7$ dyn/cm (see Appendix A).

In the region $2.0<w<4.5$ Å there is a balance between attractive and repulsive terms of the solvent–solute LJ interactions and at $w=3.02$ Å the mean force acting on the solute vanishes so that the PMF reaches a minimum. This separation may be interpreted as the distance of contact between the Ar solute particle and the solvent O atoms, since it is the smallest absolute value of w for which the mean force between Ar and O atoms is not dominated by the repulsion from the LJ core. This corresponds to configurations where water molecules have just dislodged or expelled the solute from the three-dimensional space into the fourth dimension.

Beyond $w=4.5$ Å, the PMF rises gradually with increasing w towards an asymptotic value. This rise results from the loss of long-range attractive (dispersion) interactions with the water molecules as the LJ solute is pulled out into the fourth dimension. As shown in Fig. 1, the long-range (LR) part of the PMF is found to be well fit by a function of the type $f_{\mathrm{LR}}(w)=aw^{-3}+b$. In Appendix B, we show that a can be obtained analytically in the limit of large w by integrating the dispersion interaction between the solute and a continuum solvent. For the argon LJ solute, the total dispersion coefficient defined in Eq. (B4) (see Appendix B) is $B_{\mathrm{Ar}}=947.0+2\times20.0=988.0$ kcal/mol·Å.[6] With $\rho_{\mathrm{bulk}}=0.334$ Å^{-3}, Eq. (B6) yields $V(w)=-81.42w^{-3}$. Since the PMF is defined within an arbitrary additional constant, the long-range portion of the PMF is then approximated by $f(w)=-81.42/w^3+b$, where the shift parameter b is adjusted to the $W(w)$ profile obtained from the simulation. As shown in Fig. 1, a reasonably good fit is obtained for $b=1.78$ kcal/mol.

Following Eq. (8), the hydration free energy of Argon is calculated as the PMF difference between the fully interacting state ($w=0$) and the noninteracting state ($w=\infty$), which is given by the asymptotic value of the PMF. Based on the present calculation, $\mu_{ex}=W(0)-W(\infty)=5.4-1.8=3.6$ kcal/mol.

The PMF obtained for a larger LJ sphere is shown in Fig. 2. This profile is similar qualitatively to that of the Ar solute particle. The larger size of the particle is reflected both in the larger magnitude of the free energy changes in the short-range and long-range parts of $W(w)$, and in the larger value of w_{min} for which W reaches a minimum. The analysis of the three regions of the PMF is as before. As shown in Fig. 2, the short-range ($w<3$ Å) is fit well by $f_{\mathrm{SR}}(w)=14.6-1.08w^2$, which in the framework of a phenomenological solvent-exposed area model (see Appendix A) corresponds to a surface tension of $\gamma=0.0859$ kcal/mol/Å$^2=59.7$ dyn/cm, a value close to that obtained for Ar. The minimum of the PMF occurs at $w=4.25\pm0.08$ Å. As before, this separation is the effective distance of closest approach between the solute and solvent O atoms. Finally, the long-range (LR) tail of the PMF ($w>5.5$ Å) is approximated by $f_{\mathrm{LR}}(w)=a/w^3+b$, where $a=604.5$ kcal/mol·Å^3 was calculated from the total dispersion energy of the solute particle

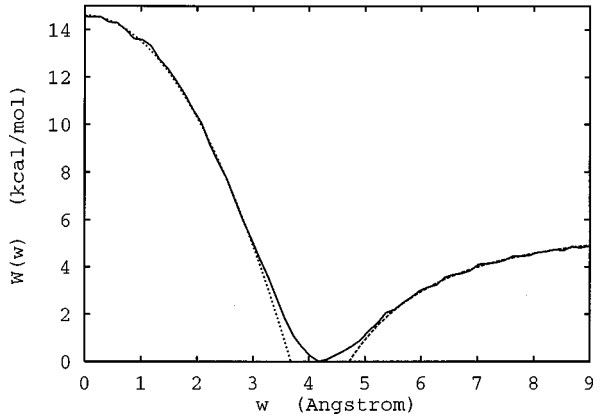

FIG. 2. (——) PMF calculated for the abstraction of the larger Lennard-Jones solute ($\epsilon = 0.190\,226$ kcal/mol, $\sigma = 4.613\,25$ Å) from water along the fourth dimension w; (----) short-range fit $f_{SR} = -1.08w^2 + 14.6$; (– – –) long-range fit $f_{LR} = -604.5w^{-3} + 5.75$.

with water (see Appendix B) and the asymptotic value $b = 5.75$ kcal/mol was obtained by fit. From this analysis we extract the value $W(0) = 14.6$ and $W(\infty) = 5.75$ kcal/mol to get $\mu = W(0) - W(\infty) = 8.9$ kcal/mol.

Water molecule

The PMF for the abstraction of a water molecule from bulk water into the fourth dimension is depicted in Fig. 3. There are three distinct regions in the profile. Unlike the LJ particles, this solute is polar, which gives rise to a qualitatively different profile. Below $|w| = 1.9$ Å, the PMF corresponds to a well centered at $w = 0$. This is because at short intermolecular separations, the solvent–solute potential energy is dominated by attractive coulombic interactions, so that work is required to extract the water solute into the fourth dimension. Besides this absolute minimum, there is a secondary free energy well at $w = 2.35$ Å. Within the 0.1 Å resolution of the histogram bins used to construct $W(w)$, the location of this minimum matches the distance of closest approach, 2.4 Å, apparent in the O–O radial distribution function for the TIP3P model.[14]

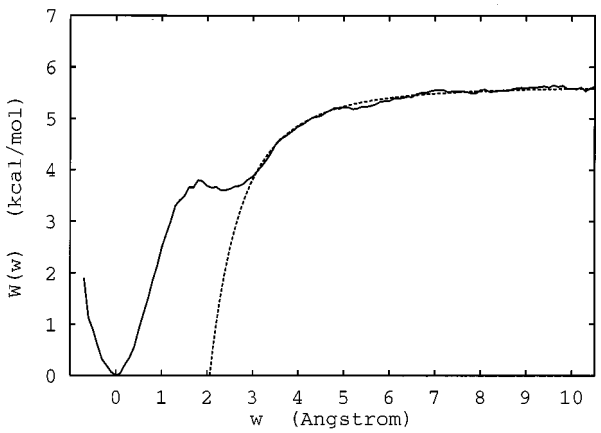

FIG. 3. (—) PMF calculated for the abstraction of a solute water molecule from TIP3P water along the fourth dimension w; (----) long-range fit $f_{LR} = -49.0w^{-3} + 5.63$.

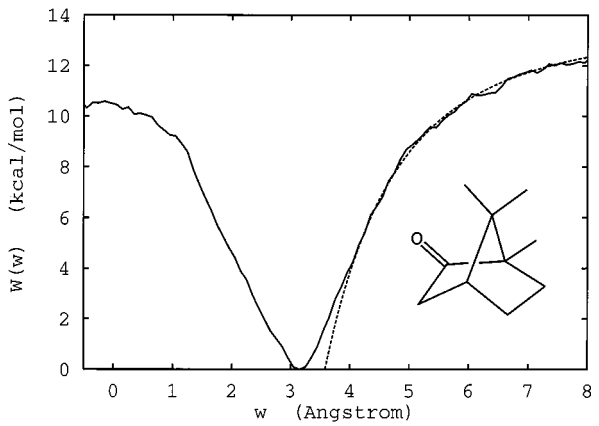

FIG. 4. (——) PMF calculated for the insertion of camphor into water along the fourth dimension w; (– – –) long-range fit $f_{LR} = -621.1w^{-3} + 13.55$. The molecular structure of camphor is depicted as an insert. The statistical uncertainty is largest in the outlying regions ($w < -0.1$ Å and $w > 8.1$ Å), which are the least sampled in the simulations.

Despite the presence of Coulombic solvent–solute interactions, the long-range tail of the water PMF is well approximated by integrating the dispersion interactions assuming a solvent continuum (Appendix B), similar to the analysis for simple LJ particles. The resulting function is $f_{LR}(w) = -49.0w^{-3} + 5.6$ kcal/mol. A derivation of the long-range contribution to the PMF arising from electrostatic interactions of the solute with water, presented in Appendix C, indicates that at separations $w \geqslant 4$ Å, the Coulombic interactions between the vanishing water molecule and bulk solvent are small (less than 3%) compared to dispersion interactions.

Consequently, the asymptotic value of W can be approximated from the long-range fit of the dispersion interactions (see Fig. 3). Based on the present calculation, the hydration free energy of TIP3P water is $\mu = W(0) - W(\infty) = 0 - 5.6 = -5.6$ kcal/mol.

Camphor

The PMF for insertion of camphor into a droplet of 251 water molecules from $w = 8$ Å to $w = 0$ Å is shown in Fig. 4. This molecule contains nine nonpolar C atoms and one polar CO group. The predominance of nonpolar centers is reflected in the qualitative profile of the PMF, which resembles that of LJ particles. Below $|w| = 3$ Å, $W(w)$ corresponds to a 10.5 kcal/mol barrier, indicating that in spite of its polarity, camphor is expelled from water. Beyond the free energy minimum at $w = 3.2 \pm 0.1$ Å, $W(w)$ is fit well by the approximation $f_{LR}(w) = -621.1/w^3 + 13.55$ where, as before, the coefficient of w^{-3} was derived from the sum of dispersion coefficients between solute and solvent atoms (see Appendix B). Overall, the long-range rise of the PMF compensates for the initial barrier, so that $W(0) - W(\infty) = 10.5 - 13.55 \simeq -3.0$ kcal/mol.

DISCUSSION

Comparison to theoretical and experimental results

We obtained values of 3.6, −5.6, and −3.0 kcal/mol for the hydration free energies of argon, water, and camphor,

respectively. In this section, we compare these results to available experimental and computational data. Because the applications presented in this study are meant as a test of the 4D-PMF method, not as a test of force fields, system size, or boundary conditions, emphasis is placed on the comparison with results obtained computationally with similar systems.

The hydration free energy of -5.6 kcal/mol that we obtained for TIP3P water in a droplet of 150 water molecules may be compared to the reported values of -5.8 and -6.4 kcal/mol calculated by λ-scaling of the potential energy in droplets of 50 and 100 TIP3P water molecules with SSBP.[16] Other results obtained for a similar three-site water potential, the single-point charge (SPC) model[21] range from -5.5 to -6.4 kcal/mol (cited in Ref. 19). The result obtained in the present study is thus within the range of other values calculated by computer simulations, and compares moderately well with the experimental value of -6.3 kcal/mol.[22] The hydration free energy of camphor was determined from experimental measurements as -3.5 kcal/mol,[23,24] a value overestimated by 0.5 kcal/mol in the present study. Given the limitations arising from the approximations inherent to the force field, such agreement is adequate.

A result of 3.0 kcal/mol was obtained for the hydration free energy of argon calculated by thermodynamic integration and free energy perturbation with λ-scaling in a droplet of 100 water molecules using identical potential functions, comparable simulation times (2 ns), and the SSBP boundary potential (M. Souaille, personal communication). This value is in fair agreement (0.6 kcal/mol, or a relative error of 20%) with our result. One source of systematic error between this calculation and our result lies in the different size of the water droplet. As noted above, previous free energy perturbation simulations using the SSBP method to calculate the hydration free energy of TIP3P water varied by 0.6 kcal/mol upon increasing the droplet size from 50 to 100 water molecules,[16] an effect similar in magnitude to the discrepancy observed here. A result of 2.0 ± 0.6 kcal/mol was obtained by free energy perturbation and thermodynamic integration for Argon with comparable LJ parameters ($\epsilon = 0.196\,478$ kcal/mol, $\sigma = 3.29$ Å) in a periodic system of SPC water molecules.[25] This disagreement, however, may be attributed largely to different water models and simulation protocols. Finally, the hydration free energy of Ar was determined experimentally as 2.0 kcal/mol.[26]

Analysis of the 4D-PMF profiles

While the chemical potentials are obtained from the limits $W(0)$ and $W(\infty)$ [see Eq. (8)], the 4D-PMF profile at intervening values of w also yields useful information. At small values of the fourth-dimensional coordinate w, expulsion of predominantly nonpolar solutes by water is reflected by the presence of a free energy barrier centered at $w = 0$. Work is required for the insertion of a solute whose interactions with water at values of w less than the contact separation are dominated by the repulsive core of the LJ potential. In the case of simple LJ spheres, the w-dependence of this barrier appears to be quadratic, which was interpreted by considering the dependence of the hydration free energy on the solute surface area, as defined by the separation between the solute and water molecules in the three physical dimensions x, y, and z (Appendix A). For the two LJ particles considered in this work, apparent surface tensions of 54.7 and 59.7 dyn/cm were derived by this analysis. Both values fall within the range of 40–60 dyn/cm obtained in a recent study of LJ solutes by extensive computer simulations.[27,28] In contrast, for a polar solute such as water, the PMF adopts the shape of a *well* at small w values. For polyatomic solutes such as camphor, the short-range PMF is a barrier, reflecting expulsion of the predominantly nonpolar groups of the solute from water. However, the dependence of this barrier is not quadratic, which arises both from the competition of Coulombic interactions and from the molecularity of the solute.

The location of the minimum in the 4D-PMF of simple LJ solutes corresponds to the distance at which the repulsive core of the hydrophobic solute has barely been expelled from the solvent. As such, this separation may be viewed as the distance of contact between the solute particle and solvent O atoms, and at which the mean attractive and repulsive forces acting on the solute cancel out exactly. In the case of the water solute, this contact minimum is a secondary one reached at $w = 2.3 \pm 0.1$ Å, a value which is consistent with the distance of closest approach of ~ 2.4 Å obtained from the TIP3P O–O radial distribution function.[14] Finally, although the 4D-PMF profile of camphor is qualitatively similar to that of simple LJ solutes, due to the complex molecular nature of camphor it is not possible, *a priori*, to ascribe the location of the PMF minimum to a distance of closest approach or contact between water and any single solute atom. However, it must be noted that the location of the minimum in the 4D-PMF of camphor (3.2 Å) reflects the size of the atoms constituent of the solute, not the size of the whole molecule, which is significantly more bulky.

Beyond 1 to 2 Å from the ''distance of contact,'' in all the cases examined here, the 4D-PMF adopts a w^{-3} dependence that can be derived analytically from summing up the dispersion interactions between each solute atom and the solvent in the limit of a solvent continuum (Appendix B). In addition, a similar analysis also led to a w^{-3} dependence of electrostatic interactions for polar, neutral molecules (Appendix C). This electrostatic contribution was shown to be of much smaller magnitude than that arising from dispersion interactions in the long-range limit. The fact that these continuum approximations are valid at such small separations would be surprising in a three-dimensional system because, as indicated for example in the radial distribution function of liquid water,[14] there is still a lot of structure in the hydration shells as far as 10 Å away from any water molecule. In contrast, the 4D-PMF of water (Fig. 3) suggests that the continuum approximation is valid at values of w as small as 3 to 4 Å—barely beyond the first hydration shell of 3D water. This difference arises from the fact that once the repulsive core of all the solute atoms has been expelled from the solvent, the influence of the solute on the local structure of the solvent largely vanishes, so that the notion of hydration shells does no longer apply as the solute takes off in the fourth dimension.

The magnitude of deviations of the 4D-PMF from the analytical short- and long-range fits f_{SR} and f_{LR} in the re-

spective regions of validity of these approximations provides an estimate of the statistical errors in the PMF profiles. From Figs. 1–4, these deviations are seen to be within 0.3 kcal/mol for Ar and camphor, within 0.2 kcal/mol for water, and within 0.1 kcal/mol for the large LJ solute. In the light of systematic errors arising from the force field and from boundary conditions, this uncertainty is acceptable and suggests that the 4D-PMF has converged adequately. Such well-behaved convergence in the limit of ''large'' values of w demonstrates the validity of the approximation as well as the reliability of the method as the solute is pulled into the fourth dimension beyond contact separation. This predictability also suggests a straightforward improvement to the computational efficiency of the method: Instead of extending the simulations all the way to (or starting from) $w=10\text{Å}$, one can save up to 50% of the CPU time by truncating the calculation of the PMF at values of w just large enough to fit the long-range PMF with confidence. In the applications presented above, these values could be 6 to 7 Å for argon and the large LJ solute, 5 Å for water, and 4.5 to 5 Å for camphor.

Applicability and advantages of the 4D-PMF method

Excess chemical potentials are calculated as the difference in the free energy of two states: Fully interacting and noninteracting solvent and solute. The specificity of the 4D-PMF method is to treat the noninteracting state as a system in which solvent and solute are infinitely separated in a nonphysical spatial dimension. This procedure is formally analogous to the ''shifting'' of solvent–solute interactions.[5,6] With both methods, numerical instabilities originating from the growth or deletion of LJ atoms with simple λ-scaling of the LJ interactions are completely avoided. In that respect, the effectiveness of shifting the nonbonded interaction potential by the extension of the solute into the fourth spatial dimension is similar to methods using shifting.[5,6] Unlike these approaches, in which the extension of solvent–solute separations is parametric [see Eq. (2)], in the 4D-PMF approach the extension is governed by the mean force exerted by the solvent on the solute along a continuous spatial dimension. In the previous discussion, we have considered how far the calculation of the PMF should extend into the fourth dimension to allow an accurate estimate of the free energy of the noninteracting state, $W(\infty)$, relative to that of the fully interacting one, $W(0)$. Importantly, the analysis of the factors governing the 4D-PMF profiles leads to physical insight of practical use. In particular, we have seen that the long-range approximation of the 4D-PMF derived from a continuum treatment of the solvent can be used advantageously, both to calculate the asymptotic value $W(\infty)$ without introducing additional errors, and to gauge the convergence of the calculations. Thus the truncation of the 4D-PMF profiles computed in this study at $w=5$ to 7 Å would lead to equally reliable estimates of $W(\infty)$. Moreover, the values of w from which the long-range approximations become valid ($w>3$ to 5 Å) are determined by atomic size (as discussed above), and do not depend on the molecular size of the solute. Accordingly, the convergence of computations of the 4D-PMF was seen to be as fast for large solutes (such as our larger LJ sphere and camphor) as for smaller ones.

To underscore further the tractability, simplicity, and generality of the 4D-PMF method, we note that unlike previously reported calculations using shifting,[5,6] the present calculations were performed without concurrent λ- or λ^n-scaling of the nonbonded interactions. The PMF approach allows to treat molecular solutes in a single set of umbrella-sampling simulations, which saves setup and analysis time. Thus the 4D-PMF results reported for camphor were obtained within one work-day, including CPU time (on four R10 000 processors) and manpower.

Based on the present study, we expect that similar simulation protocols and simulation times could be applied with confidence to a wide range of uncharged solute molecules, whether polar, or nonpolar. The case of ionic solutes will be treated in subsequent studies. In such cases, additional calculations might be needed due to the divergence of Coulombic interactions. Among the possible approaches, the insertion of a neutral analog of the solute could be treated with this method, whereas the free energy of charging or uncharging the fully inserted solute (at $w=0$) could be performed by direct free energy perturbation, by continuum electrostatic calculation,[29] or by using cumulant expansions of the derivative of the free energy with respect to the ionic charge.[30] Finally, it should be stressed that the direct application of the approach to problems of molecular recognition and ligand binding is straightforward, although simulations may need to include comparatively large values of w since the simple analytical treatment of long-range interactions derived in Appendices B and C for homogeneous media is expected to break down. In any event, it is hoped that the 4D-PMF method to compute excess chemical potentials can be of practical use in industrial and drug-design efforts.

CONCLUSIONS

We have introduced a method for the calculation of excess chemical potentials by computer simulations. We have shown how the excess chemical potential of a solute or ligand can be calculated from the PMF for abstracting the molecule into (or inserting it from) an extra spatial dimension. This approach is formally related to the parametric shifting of interatomic distances in the calculation of LJ potential interactions,[5,6] and possesses the same basic advantage over conventional free energy calculations: because the singularity problem that arises from a simple scaling of the LJ core is avoided, the method is not limited to conservative, atom-by-atom perturbations of the molecule of interest. Instead, whole molecules can be introduced or abstracted in a single set of simulations with minimal human intervention.

The tractability, simplicity, effectiveness, and generality of the method were illustrated through calculations of the hydration free energy of two LJ spheres, of water, and of camphor using molecular-dynamics simulations and umbrella sampling. We expect the method to be useful for the efficient calculation of chemical potentials of solute and ligand molecules with a wide range of sizes, shapes, and polarities. Further, in homogeneous systems it is possible to obtain a 30%–50% gain in computational efficiency by making use of the analytical integration of long-range interac-

tions between solvent and solute atoms in the limit of a solvent continuum.

Other, straightforward applications of the method could include the concerted insertion–abstraction of several molecules, for example, in computing the binding free energy of water in protein cavities.[2,8] The method can also be extended to the direct calculation of relative binding free energies by making use of negative as well as positive values of the fourth dimension w: Thus, a molecule initially at $w=0$ could be dislodged from a binding site by expelling it to $w>0$ while simultaneously bringing another ligand from $w<0$ to $w=0$. Furthermore, an effective treatment of competitive ligand binding problems could be devised through the introduction of additional (fifth, sixth, etc.) spatial dimensions, each of them reserved to a different ligand.

APPENDICES: INTERPRETATION OF THE PMF PROFILES. APPENDIX A: APPROXIMATION OF SHORT-RANGE LJ INTERACTIONS

The hydration free energy of hydrophobic solutes, μ, can be related to their solvent-exposed surface area S through a proportionality constant

$$\mu=\gamma S, \tag{A1}$$

where γ is the apparent surface tension of the solvent.[31] For simple LJ particles in water, the effective surface is defined by the distance of closest approach R_{contact} as

$$S=4\pi R_{\text{contact}}^2. \tag{A2}$$

As the solute is pulled into the fourth dimension, however, a constant contact separation in 4D corresponds to a diminishing effective 3D radius given by

$$R_{3,\text{eff}}=(R_{\text{contact}}^2-w^2)^{(1/2)}, \tag{A3}$$

so that the effective surface area of the solute at $-R_{\text{contact}} \leqslant w \leqslant R_{\text{contact}}$ becomes

$$S=4\pi R_{3,\text{eff}}^2=4\pi(R_{\text{contact}}^2-w^2). \tag{A4}$$

From the combination of Eqs. (A1) and (A4), the short-range dependence of the PMF for the expulsion of a LJ solute into the fourth dimension is predicted to be a quadratic barrier

$$W(w)=-4\pi\gamma w^2+C. \tag{A5}$$

APPENDIX B: APPROXIMATION OF LONG-RANGE LJ INTERACTIONS

In this section, we derive an analytical approximation for long-range dispersion interactions of the solute in the four spatial dimensions based on a continuum treatment of the solvent. First, we rewrite the LJ interaction potential between solvent and solute atoms i and j separated by $R_4^{ij}=(r_{ij}^2+w^2)^{(1/2)}$ as

$$V_{\text{LJ}}^{ij}(r_{ij},w)=\frac{A_{ij}}{(r_{ij}^2+w^2)^6}-\frac{B_{ij}}{(r_{ij}^2+w^2)^3}, \tag{B1}$$

with $A_{ij}=4\epsilon_{ij}\sigma_{ij}^{12}$ and $B_{ij}=4\epsilon_{ij}\sigma_{ij}^{6}$. The LJ interaction energy between the N solvent atoms and solute atom j is given by

$$V(\mathbf{r}_1,\ldots,\mathbf{r}_N,\mathbf{r}_u^{(j)},w)=\sum_{i=1}^{N} V_{\text{LJ}}^{ij}(r_{ij},w). \tag{B2}$$

In the limit of large w we approximate the solvent as a continuum. The potential is dominated by the dispersion term, whereas the repulsive term becomes negligible. By integration over the full range of 3D separations r and summation over all the atoms of the solute, Eq. (B2) becomes

$$V\simeq V(w)=\sum_j \int_0^\infty \frac{-B_j}{(r^2+w^2)^3}\rho_{\text{bulk}}4\pi r^2 dr, \tag{B3}$$

where ρ_{bulk} is the bulk density of the solvent, and

$$B_j=B_{\text{O}j}+2B_{\text{H}j}, \tag{B4}$$

is the sum of the dispersion coefficients between the solute atom j, and the atoms of a water molecule. Eq. (B3) yields

$$V(w)=-4\pi\sum_j B_j\rho_{\text{bulk}}\left[\frac{r}{4(r^2+w^2)^2}-\frac{r}{8w^2(r^2+w^2)}-\frac{\arctan(r/w)}{8w^3}\right]_0^\infty. \tag{B5}$$

Finally, for sufficiently large w, this becomes

$$V(w)=\frac{-\pi^2\rho_{\text{bulk}}\Sigma_j B_j}{4w^3}. \tag{B6}$$

APPENDIX C: APPROXIMATION OF LONG-RANGE ELECTROSTATIC INTERACTIONS

We first consider the long range tail of solvent–solute interactions in the case of a mono-atomic solute carrying a charge Q. When the solute is located at w, the electrostatic potential seen by the solvent atoms is

$$\phi(\mathbf{r})=\frac{Q}{(r^2+w^2)^{1/2}}, \tag{C1}$$

where $r=|\mathbf{r}|$. The reversible electrostatic work to charge the mono-atomic solute at a position w is expressed as a thermodynamic integral

$$V_{\text{elec}}=\int_0^Q dQ'\int d\mathbf{r}\frac{1}{(r^2+w^2)^{1/2}}\langle\rho_{\mathbf{v}}(\mathbf{r};Q')\rangle, \tag{C2}$$

where $\langle\rho_{\mathbf{v}}(\mathbf{r};Q')\rangle$ is the average charge density of the solvent (in the three-dimensional space) induced by the presence of the solute in the system. To estimate $\langle\rho_{\mathbf{v}}(\mathbf{r};Q')\rangle$ we use a continuum electrostatic approximation. The solution to this problem is particularly simple if w is larger than the range of the solute–solvent core repulsion potential because the solvent dielectric constant is uniform everywhere in the three-dimensional space. According to Poisson's equation for macroscopic media, the average solvent charge distribution induced by a solute of charge Q in a medium of dielectric constant ϵ_D is

$$\langle \rho_{\mathbf{v}}(\mathbf{r};Q)\rangle = \left(\frac{1}{\epsilon_D}-1\right)\left(\frac{-1}{4\pi}\right)\nabla^2\phi(\mathbf{r}) = \left(\frac{1}{\epsilon_D}-1\right)\frac{3Qw^2}{4\pi(r^2+w^2)^{5/2}}. \quad \text{(C3)}$$

Therefore, according to Eq. (C2)

$$V_{\text{elec}} = \frac{Q^2}{2}\left(\frac{1}{\epsilon_D}-1\right)4\pi\int_0^\infty r^2 dr\left(\frac{1}{(r^2+w^2)^{1/2}}\right) \times\left(\frac{3w^2}{4\pi(r^2+w^2)^{5/2}}\right) = Q^2\left(\frac{1}{\epsilon_D}-1\right)\frac{3\pi}{32w}. \quad \text{(C4)}$$

Following a similar approach, we now estimate the long-range electrostatic tail in the case of neutral polar solutes. The reversible work to bring the polar solute from infinity to a position w is (assuming linear response of the dielectric medium)

$$V_{\text{elec}} = \frac{1}{2}\int d\mathbf{r}\sum_{ij}\frac{Q_i}{((\mathbf{r}-\mathbf{r}_i)^2+w^2)^{1/2}}\langle \rho_{\mathbf{v}}(\mathbf{r}-\mathbf{r}_j;Q_j)\rangle, \quad \text{(C5)}$$

where $\langle \rho_{\mathbf{v}}(\mathbf{r}-\mathbf{r}_j;Q_j)\rangle$ is the average charge density of the solvent induced by the jth charge of the solute located at $\mathbf{r}_j$. Using the translational symmetry of the system, the integral is re-written as

$$V_{\text{elec}} = \frac{1}{2}\left(\frac{1}{\epsilon_D}-1\right)\sum_{ij} Q_iQ_j\int_0^{2\pi}d\phi\int_1^{\pi}d\theta\sin(\theta) \times\int_0^\infty r^2 dr\left(\frac{1}{(r^2+w^2+r_{ij}^2-2rr_{ij}\cos(\theta))^{1/2}}\right) \times\left(\frac{3w^2}{4\pi(r^2+w^2)^{5/2}}\right), \quad \text{(C6)}$$

where $r_{ij}=|\mathbf{r}_i-\mathbf{r}_j|$. To obtain the asymptotic behavior in w it is appropriate to perform a series expansion in terms of the solute intramolecular charge–charge distance r_{ij}. Retaining only the lowest nonvanishing order in r_{ij}, it is possible to express the result in terms of the solute dipole moment μ_e using the relation $\mu^2=\Sigma_{ij}Q_iQ_jr_{ij}^2$

$$V_{\text{elec}} = \frac{1}{2}\mu_e^2\left(\frac{1}{\epsilon_D}-1\right)\int_0^{2\pi}d\phi\int_1^{\pi}d\theta\sin(\theta) \times\int_0^\infty r^2 dr\,\frac{3w^2(r^2+w^2-3r^2\cos(\theta)^2)}{(8\pi(r^2+w^2)^5)} = \mu_e^2\left(\frac{1}{\epsilon_D}-1\right)\frac{15}{1024w^3}. \quad \text{(C7)}$$

As expected, the magnitude of V_{elec} becomes vanishingly small as w goes to infinity. Interestingly, the w-dependence of V_{elec} is the same as that of V_{vdw}. For a water solute in water, $\mu_e=0.5e\cdot\text{Å}$, $\epsilon_D=80$, yielding $V_{\text{elec}} = -1.200\,623/w^3\ \text{kcal}\cdot\text{mol}^{-1}\cdot\text{Å}^3$. This is much smaller than the correction for the van der Waals long range tail ($-49.0/w^3\ \text{kcal}\cdot\text{mol}^{-1}\cdot\text{Å}^3$, see Appendix B).

ACKNOWLEDGMENTS

We wish to thank Marc Souaille for communicating unpublished results and Shekhar Garde for stimulating discussions. This work was supported in parts by a grant from the Medical Research Council of Canada, by the U.S. Department of Energy through the Los Alamos National Laboratory LDRD-CD grants for Bioremediation, and by Grant Nos. NIH-AI39639 and NIH-GM39478. B.R. is a research fellow of the Medical Research Council of Canada.

[1] D. Frenkel and B. Smit, *Understanding Molecular Simulation: From Algorithms to Applications* (Academic, San Diego, 1996).
[2] B. Roux, M. Nina, R. Pomès, and J. C. Smith, Biophys. J. **71**, 670 (1996).
[3] M. K. Gilson, J. A. Given, B. L. Bush, and J. A. McCammon, Biophys. J. **72**, 1047 (1997).
[4] T. Simonson, Mol. Phys. **80**, 441 (1993).
[5] T. C. Beutler, A. E. Mark, R. C. van Schaik, P. R. Gerber, and W. F. van Gunsteren, Chem. Phys. Lett. **222**, 529 (1994).
[6] M. Zacharias, T. P. Straatsma, and J. A. McCammon, J. Chem. Phys. **100**, 9025 (1994).
[7] T. C. Beutler and W. F. van Gunsteren, J. Chem. Phys. **101**, 1417 (1994).
[8] V. Helms and R. C. Wade, J. Am. Chem. Soc. **120**, 2710 (1998).
[9] R. C. van Schaik, H. J. C. Berendsen, A. E. Torda, and W. F. van Gunsteren, J. Mol. Biol. **234**, 751 (1993).
[10] X. Kong and C. L. Brooks, III, J. Chem. Phys. **105**, 2414 (1996).
[11] Z. Guo and C. L. Brooks, III, J. Am. Chem. Soc. **120**, 1920 (1998).
[12] Z. Guo, C. L. Brooks, III, and X. Kong, J. Phys. Chem. B **102**, 2032 (1998).
[13] B. R. Brooks, R. E. Bruccoleri, B. D. Olafson, D. J. States, S. Swaminathan, and M. Karplus, J. Comput. Chem. **4**, 187 (1983).
[14] W. L. Jorgensen, J. Chandrasekhar, J. D. Madura, R. W. Impey, and M. L. Klein, J. Chem. Phys. **79**, 926 (1983).
[15] G. C. Maitland, M. Rigby, E. B. Smith, and W. A. Wakeham, *Intermolecular forces: Their Origin and Determination* (Clarendon, Oxford, 1981).
[16] D. Beglov and B. Roux, J. Chem. Phys. **100**, 9050 (1994).
[17] S. Kumar, D. Bouzida, R. H. Swendsen, P. A. Kollman, and J. M. Rosenberg, J. Comput. Chem. **13**, 1011 (1992).
[18] B. Roux, Comput. Phys. Commun. **91**, 275 (1995).
[19] V. Helms and R. C. Wade, Biophys. J. **69**, 810 (1995).
[20] A. D. Mackerell Jr., D. Bashford, M. Bellot, R. L. Dunbrack, J. D. Evanseck, M. J. Field, S. Fischer, J. Gao, H. Guo, S. Ha, D. Joseph-McCarthy, L. Kuchnir, K. Kuczera, F. T. K. Lau, C. Mattos, S. Michnick, T. Ngo, D. T. Nguyen, B. Prodhom, W. E. Reither, III, B. Roux, M. Schlenkrich, J. C. Smith, R. Stote, J. Straub, M. Watanabe, J. Wiórkiewicz-Kuczera, and M. Karplus, J. Phys. Chem. B **102**, 3586 (1998).
[21] H. J. C. Berendsen, J. P. M. Postma, W. F. van Gunsteren, and J. Hermans, in *Intermolecular Forces*, edited by B. Pullman (Reidel, Dordrecht, 1981).
[22] A. Ben-Naim and Y. Marcus, J. Chem. Phys. **81**, 2016 (1984).
[23] N. Ishizaka, Naunyn-Schmiedebergs Arch. Exp. Pathol. Pharmakol. **75**, 194 (1914).
[24] M. P. Datin, Ann. Phys. (Paris) **5**, 218 (1916).
[25] T. P. Straatsma, H. J. C. Berendsen, and J. P. M. Postma, J. Chem. Phys. **85**, 6720 (1986).
[26] E. Wilhelm, R. Battino, and R. J. Wilcock, Chem. Rev. **77**, 219 (1977).
[27] G. Hummer and S. Garde, Phys. Rev. Lett. **80**, 4193 (1998).
[28] We note that invoking phenomenological surface tension models for calculating hydration free energies of microscopic solutes should be done with caution. In particular, using the values of apparent surface tensions obtained here for simple spherical solutes might not be appropriate for complex molecular solutes. In the case of hydrophobic solutes molecules, using information theory to model density fluctuations in water could provide a more promising alternative. See for example G. Hummer, S. Garde, A. E. García, M. E. Paulaitis, and L. R. Pratt, J. Phys. Chem. B **102**, 10469 (1998).
[29] M. Nina, D. Beglov, and B. Roux, J. Phys. Chem. B **101**, 5239 (1997).
[30] S. Garde, G. Hummer, and M. E. Paulaitis, J. Chem. Phys. **108**, 1552 (1998).
[31] H. Reiss, H. L. Frisch, and J. L. Lebowitz, J. Chem. Phys. **31**, 369 (1959).